Humidity modulated surface pattering of large-scale molecular ferroelectric thin films based on natural alkaloids

Mia Mesić and Lidija Androš Dubraja*

Ruđer Bošković Institute, Bijenička cesta 54, 10000 Zagreb, Croatia

Dr. Lidija Androš Dubraja

Ruđer Bošković Institute

Bijenička cesta 54

10000 Zagreb, Croatia

Tel.: +385 1 4561-184

Fax: +385 1 4680-098

E-mail: Lidija.Andros@irb.hr

Abstract

Molecular ferroelectrics with low power consumption offer environmental and economic advantages over conventional ferroelectrics and could lead to next-generation microelectronic devices. To this end, it is of great importance to understand the conditions under which molecules can be engineered to form large-area, highly oriented thin films, as their electrical properties depend on orientation. In the research field of molecular ferroelectrics, homochiral multifunctional organic molecules are often used to induce the self-assembly of molecules through non-covalent interactions to form polar crystal packings and consequently ferroelectric properties. Here, molecular ferroelectric thin films based on the natural Cinchona alkaloid, cinchoninium cation and chlorocobaltate(II) anion were prepared by a dip-coating technique without post-thermal treatment and assisted stabilization process. The deposition parameters (relative humidity, temperature, concentration and withdrawal speed) were modified to produce either completely dense or fully patterned films with randomly distributed holes on the surfaces. While non-covalent interactions are the main factor in determining the structure of cinchoninium-trichloro-cobalt(II) thin films, relative humidity is a key parameter in the simultaneous self-organization happening at the mesoscale, acting as a dewetting agent. Dense cinchoninium-trichloro-cobalt(II) films exhibit a stable ferroelectric switching at a low operating voltage, and patterned films were tested as resistive methanol sensors.

Keywords

metal-organic, thin film, dip-coating, *Cinchona* alkaloids, dewetting, molecular ferroelectric; methanol sensing

1. Introduction

Molecular ferroelectrics are attracting considerable attention as an environmentally friendly, economical and biocompatible alternative to conventional hard ferroelectrics, mainly because their ferroelectric properties are nowadays approaching those of their inorganic counterparts [1–3]. In addition to mechanical flexibility and low weight, the synthesis of molecular ferroelectrics, which is based on soft and mild methods, mostly via coordination and supramolecular chemistry, is one of the outstanding advantages over conventional ferroelectrics [4]. Due to the high content of organic components, the total mass fraction of metals, which are often expensive and scarce, is much lower in molecular ferroelectrics, and they can be recovered or recycled by simple dissolution [5]. Furthermore, the properties of molecular ferroelectrics, such as spontaneous polarization [6], coercive field [7] or phase transition temperature [8], can be controlled by chemical design due to their structural and compositional tunability. These advantages make molecular ferroelectrics promising alternatives for future electronic devices [9].

The most common approach to construct homochiral architectures with potential ferroelectric properties is the rational combination of chiral organic ligands as linkers and metal ion nodes with a specific coordination geometry [10,11]. Multifunctional organic ligands with several donor and acceptor sites are common structural motifs that can facilitate crystal engineering and performance optimization of molecular ferroelectrics [12]. However, the complexity of ligand synthesis limits the engineering of size, flexibility, and directionality of binding centers [13]. A synthetic strategy that focuses on the use of naturally occurring chiral ligands may be an effective route to fabricating molecular ferroelectrics.

Readily accessible *Cinchona* alkaloids are naturally occurring compounds extracted from the bark of *Cinchona* pubescens [14]. The alkaloids mainly contain quinine, its quasi-enantiomer quinidine and their analogs without a methoxy group in the quinoline ring, cinchonidine and cinchonine, respectively [15]. The alkaloids and their derivatives have been intensively studied from the point of view of medicinal applications [16], enantioselective catalysis and separation [17], rather than as chiral building blocks for metal–organic supramolecular architectures [18]. In addition to the aromatic system, *Cinchona* alkaloids contain the polar quinuclidine fragment, which is responsible for the ferroelectric effect in many molecular ferroelectrics due to its rotational properties [19–21]. To develop functional materials based on *Cinchona*

alkaloids, it is necessary to understand at the molecular level the supramolecular forces that govern the self-assembly of the associated complexes, which the crystal structure gives the best insight into [22].

From the point of view of manufacturing electronic devices, the formation of defect-free, thin, stable and continuous thin films on a variety of substrates without substrate modification is extremely important [23]. Molecular thin films can be fabricated at large scale under mild conditions using low-temperature solution-based techniques, making them good candidates for the next generation of flexible, lightweight, compact and integrated electronic devices [1,6,23]. Compared to bulk samples, ferroelectric thin films operate at lower voltages, faster speeds and unique submicron structures [24].

Although solution-processable molecules can be deposited cost-effectively on various substrates by dip coating [25], spin coating [26], or inkjet printing [27], the production of high-quality thin films with smooth surfaces is still a major challenge. The morphology, thickness and crystallinity of solution-fabricated films are influenced by the synergistic effect of many different parameters that need to be optimized during deposition, such as solution preparation (*e.g.* solvent combination, concentration) [28], substrate choice (*e.g.* wettability, smoothness) [29] and environmental conditions (*e.g.* relative humidity, temperature) [30]. The solubility of metal-organic molecules (especially ionic crystals) can be used to prepare suitable solutions which enable the deposition of thin films or, in some cases, colloidal suspensions can be used [31,32]. Recently, it has been shown that nanostructured, high-quality thin films of $Fe_xO/CoFe_2O_4$ core/shell nanocrystals can be produced using the dip-coating method [32]. In these thin films, properties such as organization, uniformity and thickness can be adjusted by varying the solvent, concentration, substrate surface treatment and withdrawal speed [32].

Herein, a comprehensive investigation on the direct preparation of high-quality molecular ferroelectric thin films of cinchoninium-trichloro-cobalt(II) complex, $CnCoCl_3$, (cinchoninium, Cn = $C_{19}H_{23}N_2O$) by dip-coating on various substrates is presented. In this molecular ferroelectric, the self-assembly of molecules driven by intermolecular interactions leads to the formation of crystalline thin films with controllable preferred orientation. *In-situ* control over the deposition parameters enables self-organization and spontaneous pattern formation during solvent evaporation. The formation of a similar arrangement of holes or droplets was first reported by Reiter during the *ex-situ* annealing of polystyrene thin films and attributed to

the dewetting process of unstable films [33,34]. Since then, the reasons for the formation of almost regular hole patterns in thin films have not been fully addressed, mainly due to system differences [35–38]. In this work, the formation of fully dense to patterned large-area molecular ferroelectric thin films of $CnCoCl_3$ complex is described in detail and a correlation between the structure, morphology and (ferro)electric performance is established.

2. Material and methods

2.1. Starting Materials

Cinchoninium chloride dihydrate (85%), $CnCl{\cdot}2H_2O$, was purchased from Sigma Aldrich and cobalt(II) chloride hexahydrate (98%), $CoCl_2{\cdot}6H_2O$, was purchased from Alfa Aesar. Si(100) substrates were purchased from Siegert wafer GmbH. Ultra-flat quartz and indium-doped tin oxide (ITO) coated glass substrates were purchased from Ossila BV.

2.2. Synthesis of $CnCoCl_3$

$CnCl{\cdot}2H_2O$ (*m* = 92 mg; *n* = 0.25 mmol) and $CoCl_2{\cdot}$(*m* = 65 mg; *n* = 0.5 mmol) were dissolved in methanol and subsequently the solutions were mixed. Blue prism-like single crystals of cinchoninium-trichloro-cobalt(II) complex, $CnCoCl_3$, formed within a day. Anal. Calcd % for $C_{19}H_{23}N_2OCoCl_3$ (found, %): C, 49.53 (49.75); H, 5.03 (5.52); N, 6.08 (6.22); Co, 12.79 (12.96); Cl, 23.08 (23.58). Crystals were separated by filtration and used as such for preparation of thin films.

2.3. Thin film deposition

For the fabrication of thin films, $CnCoCl_3$ (*m* =27 mg ; *n* = 0.06 mmol) was dissolved in a solvent mixture of methanol (3 mL) and acetonitrile (3 mL). Thin films were prepared by dip-coating on Si(100), ITO-coated glass, ultra-flat quartz and polypropylene substrates in a humidity-controlled chamber. During the deposition of films different parameters were varied, such as withdrawal rate, relative humidity (RH), temperature of the chamber and drying temperature.

2.4. Physical Measurements

Attenuated total reflectance Fourier transformed infrared (ATR-FTIR) spectra were recorded in the 4000–400 cm^{-1} range using a PerkinElmer FTIR Frontier spectrometer. UV/Vis spectra were recorded using a Shimadzu UV-Vis-NIR spectrometer (model UV-3600) equipped with an integrated sphere. The single-crystal X-ray diffraction data were collected by ω-scans using Cu-Kα radiation (λ = 1.54179 Å, microfocus tube, mirror monochromator) using a Rigaku

XtaLAB Synergy diffractometer at 293 K. The powder X-ray diffraction (PXRD) data of bulk samples and thin films were collected in reflection mode using Cu-Kα radiation (λ = 1.54060 Å) using a Malvern Panalytical Empyrean diffractometer with a step size of 0.013° in a 2ϑ range between 5° and 60°. Thermal analysis was performed with a Shimadzu DTG-60H analyser, in the range from room temperature to 1073 K, in a stream of synthetic air at a heating rate of 10 K min^{-1}. Scanning electron microscopy imaging (SEM) and energy dispersive X-ray spectroscopy (EDX) were performed on a field emission scanning electron microscope (model JSM-7000F) operated at 10 keV. The current response during exposure to methanol vapors was monitored by chronoamperometric measurements with a PalmSens4 potentiostat. Ferroelectric tests were performed using a TF Analyzer 1000 at room temperature in the frequency range of 1–10 Hz.

3. Results and discussion

3.1. Thin Film Synthesis and Structure

Cinchona alkaloid metal complexes, as homochiral constituting units, are suitable candidates for the construction of polar supramolecular architectures in the solid state. The cations of the *Cinchona* family are composed of quinolone rings, which provide stability through possible aromatic stacking interactions, and quinuclidine fragments, which provide flexibility through low-energy rotational possibilities. The chemical and thermal stability of *Cinchona* alkaloids makes them excellent and cost-effective chelating ligands for the construction of chiral metal complexes and networks [18]. To prepare the thin films of *Cinchona* alkaloid metal complexes, the metal complex was first synthesized in the bulk form from the solution of the starting reagents cinchoninium chloride and cobalt(II) chloride in appropriate ratios. The $CnCoCl_3$ complex crystallizes from such a solution in the form of blue stick-like crystals in stoichiometric yield. The structure of the material produced belongs to the polar monoclinic space group $P2_1$ [22] (details given in Supplementary data as Table S1) in which cobalt(II) adopts a tetrahedral geometry consisting of three chlorine atoms and one nitrogen atom of the quinolone ring (Figure 1a). The neutral complexes are connected by hydrogen bonds to form a three-dimensional supramolecular architecture. The strongest interaction is achieved between the hydrogen on the hydroxyl group and a chlorine atom, and this type of O–H···Cl contact is spread into infinite chain along the [001] direction (Figure 1b). Along the direction of the polar

axis there is a different type of intermolecular contact propagating, belonging to the C–H···Cl type, as shown in Figure 1c. In this direction also weak stacking π-interactions are recognized. Details related to hydrogen bonding and aromatic stacking geometry are given in Tables S2 and S3 in Supplementary data. For that reason the crystal grow into stick-like morphology with small {001} sides and elongated {100} and {020} faces. The as-made bulk material (PXRD pattern of bulk is given in Figure S1) was used to prepare the thin films of the cinchoninium-trichloro-cobalt(II) complex, $CnCoCl_3$, by a dip-coating method. Depending on the drying conditions during the preparation of the films, 298 K vs. 323 K different orientations of the films can be achieved. When $CnCoCl_3$ films are dried at room temperature, the PXRD pattern of the film on a Si(100) substrate only shows peaks at 9.5, 19.0 and 28.5, which correspond to the 00*l* reflections of the monoclinic $P2_1$ structure of the $CnCoCl_3$ complex (Figure 1d, Figure S2). When the films are placed on a hot plate at 323 K during drying process, only one diffraction peak is detected, which belongs to the 020 reflection of the monoclinic $P2_1$ structure of the $CnCoCl_3$ complex (Figure 1e, Figure S3). In both thin film samples, the diffraction peaks are of rather low intensity due to the film thickness, the predominantly organic composition with low atomic scattering factors and the fluorescence of cobalt during the PXRD measurement. In addition to these peaks, the XRD pattern shows peaks originating from the Si(100) substrate (2θ peak at 33°) [39]. Subsequent heating of the films to 423 K has no effect on the intensity or position of the peaks, confirming the thermal stability of the ferroelectric phase (TG/DTA curves given in Figure S4). A closer look at the hydrogen bonds provides a possible explanation for the observed preferential growth of the films. At room temperature, the molecules arrange in the most energetically favorable way, namely along the [001] direction in which the shortest type of intermolecular hydrogen bonding propagates. As the drying temperature increases, more energy is added to the system, causing the molecules to arrange along the direction of the polar axis in which the weaker C–H···Cl and π-stacking contacts propagate. The influence of temperature on the specific directional growth of metal-organic thin films was observed in a compound containing copper ions and 2,3,6,7,10,11-hexahydroxytriphenylene ligands [40]. In this metal-organic framework, two orientations along the [001] and [100] directions can be achieved by changing the types of solvents (ethanol vs. water) and the reaction temperature (312 vs. 343 K) during the preparation process. The observation that the drying temperature during the evaporation process has a significant effect on the growth of the cinchoninium-trichloro-cobalt(II) thin

films in a specific direction on the substrate is a direct consequence of the soft crystal packing, which in this particular case is governed by hydrogen bonding and stacking interactions.

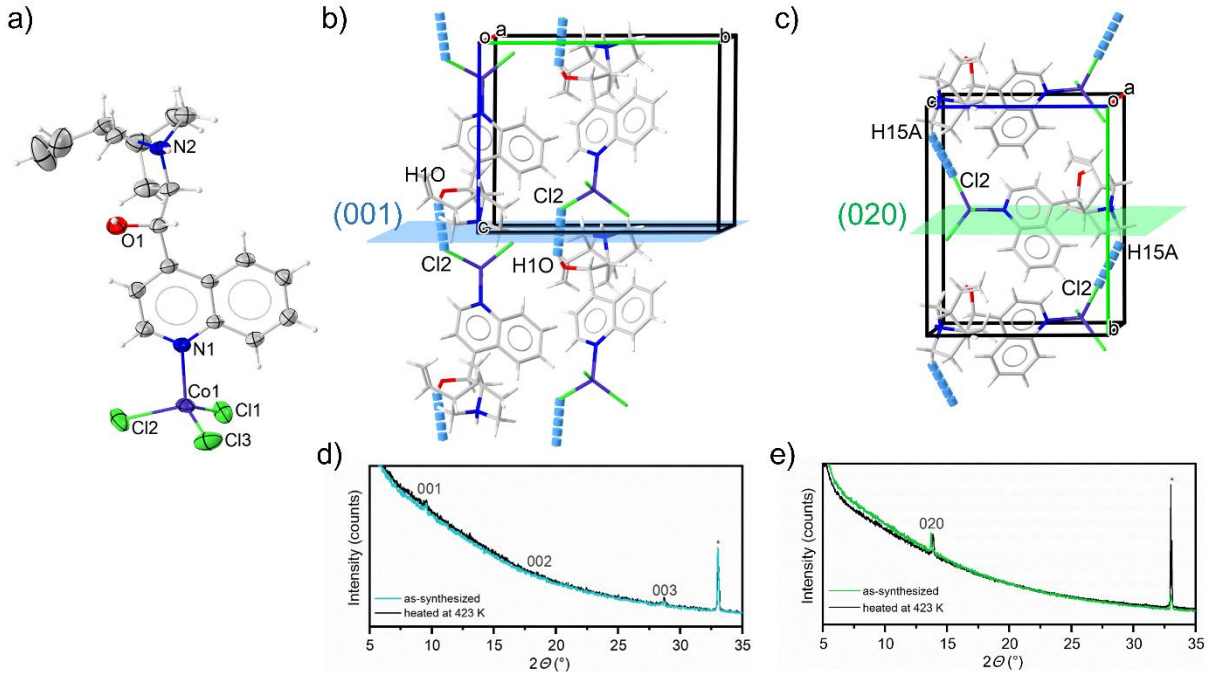

Figure 1. a) Molecular structure of the cinchoninium-trichloro-cobalt(II) complex ($CnCoCl_3$). Displacement ellipsoids are drawn with 50% probability, and hydrogen atoms are shown as spheres with arbitrary radii; b) Hydrogen bonding in $CnCoCl_3$ (blue sticks) along [001] direction; c) Hydrogen bonding in $CnCoCl_3$ (blue sticks) along [010] direction; d) PXRD pattern of $CnCoCl_3$ thin film deposited on Si(100) substrate during drying at room temperature; e) PXRD pattern of $CnCoCl_3$ thin film deposited on Si(100) substrate during drying at 323 K. The peak marked with an asterisk is from the Si substrate.

The dip-coating process is solution-based and the films are formed during withdrawal of the substrates by an evaporation-induced self-assembly process. The first step that needs to be optimized to obtain crystalline and uniform thin films is to prepare the appropriate dip-coating solution by adjusting the concentration of precursors, pH, and combination of solvents that ensure suitable viscosity and density of the solution for the coating process [31]. In the cinchoninium-trichloro-cobalt(II) system, the 0.01 M solution in a mixture of methanol and acetonitrile was optimal to obtain thin films with the desired properties. In addition to the dip-coating solution, there are other factors such as withdrawal rate, relative humidity, temperature and drying time that need to be carefully monitored and adjusted. In some cases, the substrate itself is an important factor that determines the growth of the films. In this

particular system, different substrates were used to produce thin films for different characterizations, *i.e.* Si(100), ITO/glass, ultra-flat quartz and polypropylene substrates, and films with similar properties were formed regardless of the substrate. The optical image of the $CnCoCl_3$ films shows that the thin films can be homogeneously distributed and cover the large-area substrates with the dip-coating method with some limitations (Figure 2a). Figures 2c and 2d show top-view electron micrographs of the different areas of the films shown in Figure 2a. The films produced are continuous and homogeneous and have a number of holes randomly distributed on the surface. The brown colored areas are thinner parts of the films, but their morphology is very similar to the thicker parts (multicolored area in Figure 2a). The thickness of the film is about 100 nm in the thicker part of the film, as can be seen from the cross-sectional SEM image (Figure 2b). The qualitative elemental composition was determined by energy dispersive X-ray analysis (Figure 2e) to verify the purity of the produced materials. The films show very high intensity peak related to the substrate (Si wafer) and the elements present in the $CnCoCl_3$ complex, namely Co, Cl, N, O and C, which cannot be reliably determined by EDX analysis.

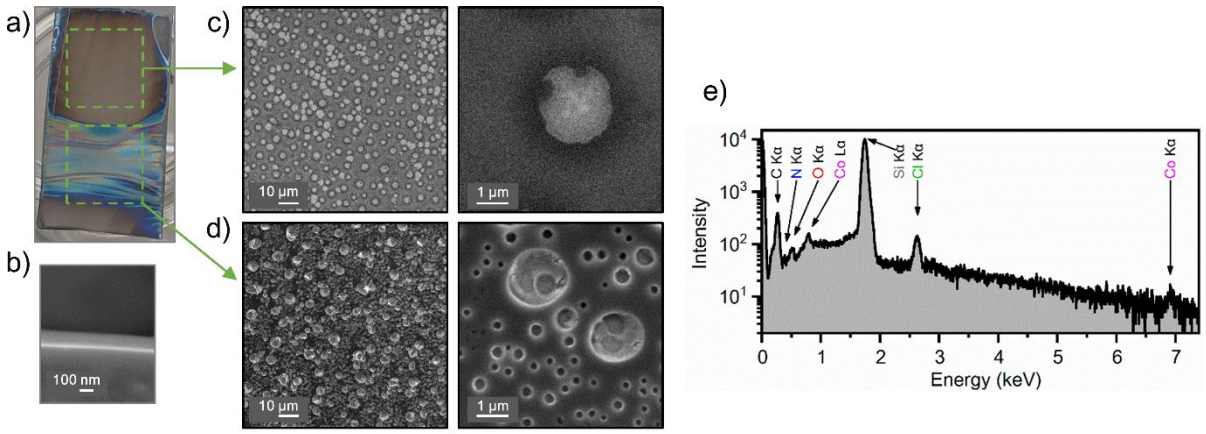

Figure 2. a) Optical image of $CnCoCl_3$ thin films on Si(100) substrate (size 1 × 2 cm) prepared by dip-coating; b) cross-sectional SEM image; c, d) top-view SEM images showing different areas on films (indicated by green square and arrow); e) EDX spectra of the corresponding thin film.

To further investigate the spectroscopic properties of the prepared films, the ATR-FTIR spectra of the films deposited on polypropylene substrates were measured (Figure 3a). The comparison between the bulk crystals and the thin films is possible for the regions in the

spectra where polypropylene shows no vibrations. The most intense bands, which can be seen in the spectra of the bulk crystals, are also found in the thin films. The bands at 3400 and 3183 cm^{-1} are related to the *ν*(O–H) and *ν*(N–H) stretching vibrations associated with the hydrogen atoms of the hydroxyl group and the protonated quinuclidine nitrogen, respectively. The most intense band in the spectra, associated with the ring deformation of the quinolone group and centered at 776 cm^{-1} [41], is present in both the bulk crystals and the thin film.

The UV/Vis spectra of the dip-coating solution used to deposit the films and the thin films deposited on quartz substrates were measured in transmission mode, while the spectra of the bulk crystals were measured in reflection mode. The electronic spectra of the solution, bulk crystals and thin films indicate cobalt(II) ions in a tetrahedral environment (Figure 3b). A triplet peak at around 650 nm is due to excitations from the ground $^4A_2$ orbital singlet to the excited $^4T_1$ orbital levels [42].

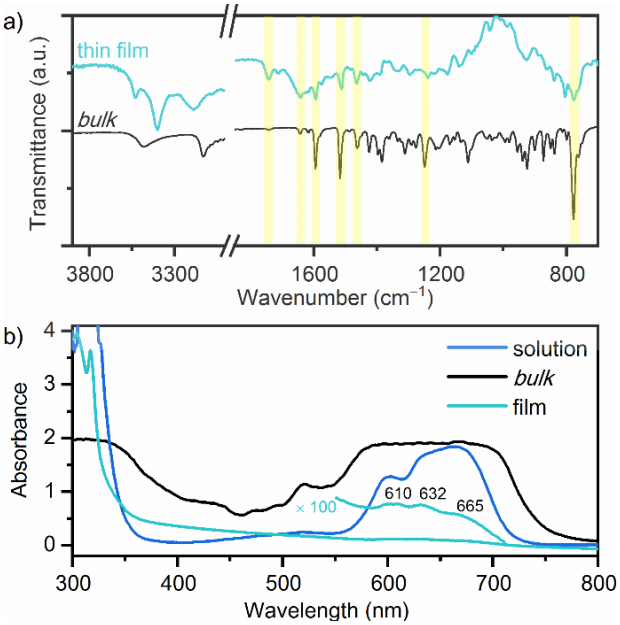

Figure 3. Spectroscopic characterization of $CnCoCl_3$: a) ATR-FTIR of thin films deposited on polypropylene substrates and bulk crystals; b) UV/Vis absorption spectra of dip-coating solution, bulk crystals and thin films.

3.2. Dewetting and morphological evolution

From the PXRD analysis and the first collected electron micrographs, it was evident that the formation of $CnCoCl_3$ thin films is determined by the self-assembly of molecules driven by non-covalent interactions and a specific pattern formation which occurs simultaneously with

evaporation. To investigate the morphological evolution of the holes that occur as a result of the apparent dewetting process that takes place *in-situ* during deposition, different parameters were varied and the electron micrographs of the produced films are shown in Figure 4. In the first experiment, the relative humidity parameter was tested and was found to have a major influence on the morphology of the thin films. At a low relative humidity of 5 %, completely dense, homogeneous and uniform thin films were formed from a 0.01 M solution at 293 K and 30 mm s^{-1} withdrawal rate. When the same experiment was carried out at an increased relative humidity of 20 %, a specific pattern formation in the form of holes was observed on the surface of the films. SEM images with higher magnification show that the size of the holes is not uniform, ranging from small holes with a diameter of 10 nm to almost 1 µm (see Figure 2d). Although the distribution of holes was completely random for most of the films, for higher withdrawal speeds (50 mm s^{-1}) a quasi-regular sequence arrangement of holes could be observed, following the vertical direction of extraction of the substrate, *i.e.* the withdrawal direction (Figure S5, Supplementary data). Another interesting observation in multilayer films, produced by multiple depositions on the same substrate is that the morphology of the holes is preserved and a plateau is formed with each deposition cycle (Figure S6, Supplementary data). Temperature of chamber for deposition could only be varied slightly due to technical issues, from 293 to 303 K, but it shows no significant influence on the pattern formation (for 0.01 M solution, 20% RH and 30 mm s^{-1} withdrawal rate). For the increased concentrations of dip-coating solution (0.01 M *vs.* 0.02 M) the formation of the films was largely accompanied by the crystallization of the bulk complex on the surface of the film, which is an unwanted process in thin film production. Another parameter that was varied was withdrawal rate, and as expected it only had impact on the thickness of films: for smaller withdrawal rates thinner films are grown [43].

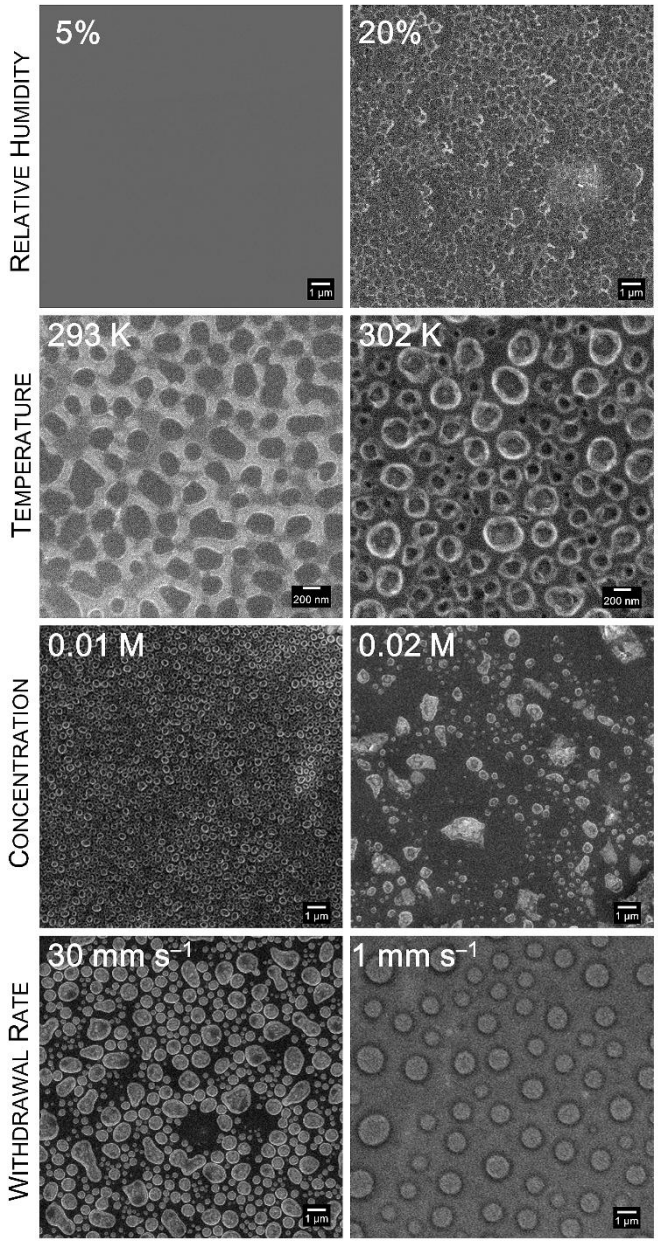

Figure 4. Electron microscopy images of $CnCoCl_3$ thin films prepared by changing the parameters during deposition: relative humidity, temperature, concentration of the precursor solution, withdrawal rate of the substrate from the precursor solution.

From the experiments performed, it can be concluded that relative humidity is an important factor for the surface structuring of $CnCoCl_3$ thin films prepared by dip-coating. Since this type of mesoscale surface patterning has not been observed in other dip-coated thin films without the use of structure directing agents or prepatterned substrates, the hole formation in $CnCoCl_3$ thin films is related to the chemical and structural properties of metal-organic system itself. Obviously, intermolecular interactions, which control crystal growth at the molecular level

propagating the hydrogen bonding in a specific crystallographic directions, also play an important role in structuring surface morphology at the mesoscale. The combination of surfaces rich in acceptor and donor sites, where polar molecules, *e.g*. water from the air, tend to form hydrogen bonds, and sufficient relative humidity leads to the formation of such specific thin films with holes. Previous work has shown experimentally that metal-organic crystals at the surface and grain boundaries have a strong tendency to bind water from the air in layers that are structured in a certain way [44]. In this type of metal-organic complex, water from the air acts as agent for phase change between hydrated and dehydrated forms in the bulk crystals. To some extent, this can be related to the processes involved in the deposition of $CnCoCl_3$ thin films, where water acts as a dewetting agent to pattern the surfaces. This may be a possible way to create ordered mesoscale surface patterns of interest in coatings technology. Recently, it has been shown that post-synthetic dewetting instabilities in nanoscopic poly(2-vinyl pyridine) films can be used to develop a form of encoded surfaces for security applications [45]. The fact that a random distribution of holes in $CnCoCl_3$ films can be achieved without post-synthetic modifications and that such specific morphology of the films is maintained under ambient conditions or at higher temperatures (at 423 K) could make these soft molecular materials useful for similar applications.

3.3. Ferroelectric properties

Organic and metal-organic single crystals often show an anisotropic molecular arrangement, consequently, charge transport depends strongly on their orientation [46]. For the integration of single crystals into devices, the control of the orientation of the single crystal is thus of importance. A very convenient approach to maximize polarization along the switching direction is to grow epitaxial ferroelectric thin films along the polar axis on appropriately selected conductive substrates [47]. Since thin films of the ferroelectric $CnCoCl_3$ phase can be grown along the direction of the two-fold rotation axis, they might be expected to exhibit out-of-plane polarization in the electric field. Calculation of the electrostatic potential on the Hirshfeld surface using the CrystalExplorer program [48] shows that the quinuclidine fragment with a low rotational energy barrier has a region of negative electrostatic potential on the surface where the ethylene fragment is located and a positive electrostatic potential on the surface where the protonated nitrogen is located (see Figure S7). If this direction is considered as the local dipole of the quinuclidine fragment, the alignment of dipoles along the direction

of polar axis is as shown on Scheme 1. In the crystal structure of $CnCoCl_3$, the ethylene group is disordered in two positions, confirming that this part of the $CnCoCl_3$ molecule exhibits flexibility and dynamics at room temperature.

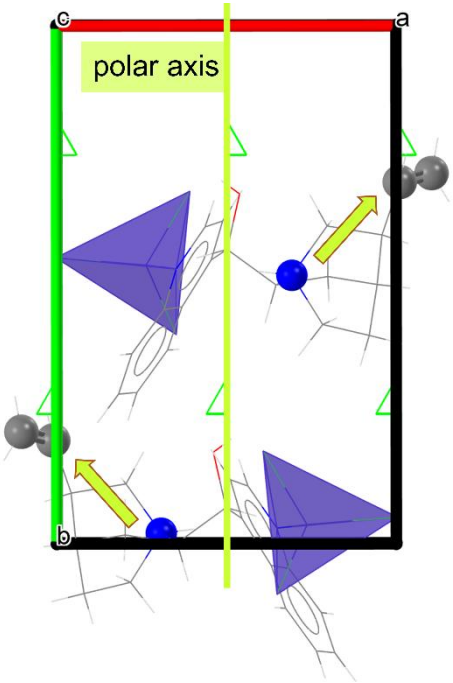

Scheme 1. Schematic representation of the arrangement of local dipole moments (represented with arrows) along the polar axis in the crystal packing of $CnCoCl_3$.

Another important feature for ferroelectric properties is to produce densely packed and homogeneously smooth surface films. For the purpose of ferroelectric testing, the 200 nm thick metal-organic films were deposited on conductive ITO/glass substrates by dip-coating from 0.01 M solution of $CnCoCl_3$ in methanol : acetonitrile (1 : 1) at a 5% RH and 323 K drying temperature. The morphology of these films is dense and free of holes on the surface of films. Gold was thermally evaporated on the top of the metal-organic film onto an area of 0.1 mm^2, which served as the top electrode. The ferroelectric properties of the as-made films investigated by polarization-electric field (*P*–*E*) measurements at room temperature (298 K) are shown in Figure 5a. To exclude the non-switching contributions (dielectric capacitance and leakage current) in this metal-organic thin film sample, a positive up-negative-down (PUND) method with a double triangular voltage pulses was used [49,50].

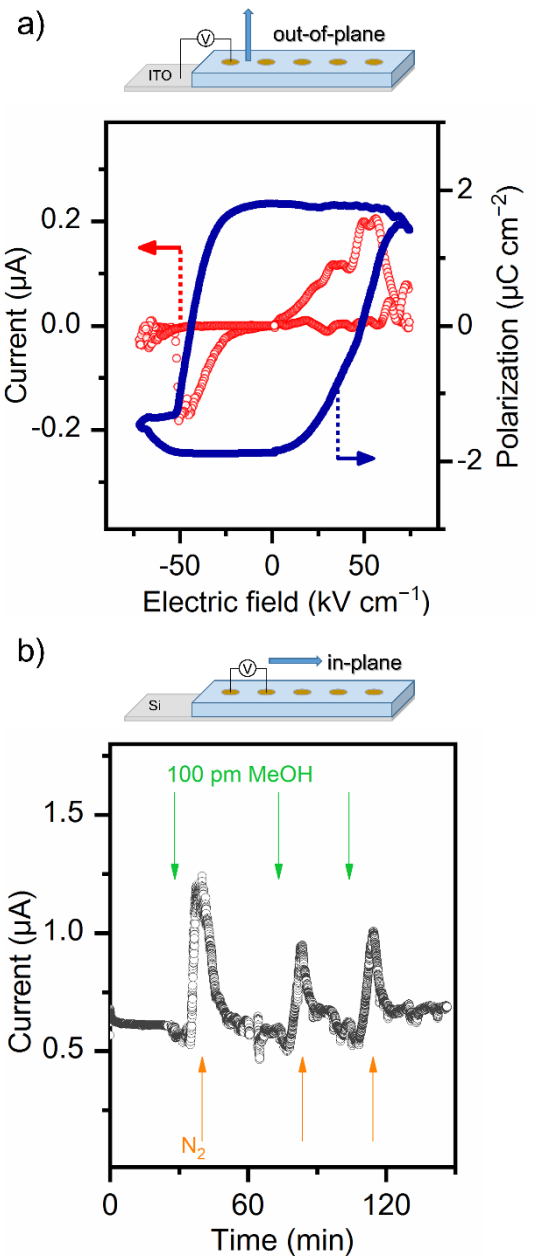

Figure 5. Electrical properties of $CnCoCl_3$ thin films: a) ferroelectric polarization and corresponding current response of $CnCoCl_3$ on ITO/glass substrate with Au top electrodes for 5 Hz switching frequency at 298 K; b) change in the current (conductivity) upon exposure to methanol vapors and dry nitrogen of the $CnCoCl_3$ thin films at 298 K and ambient pressure.

The spontaneous polarization (P_s) of $CnCoCl_3$ thin film reaches a value of ~1.8 μC cm^{-2} at a coercive field (E_c) of about 50 kV cm^{-1}, as shown in Figure 5a. Direct comparison with data on ferroelectric properties of other homochiral *Cinchona* based halogeno-copper complexes is difficult as these studies only report results from dynamic measurements in bulk samples

[20,51], which either lead to an overestimation of polarization due to presence of dielectric polarization and leakage current, or its underestimation due to difficulties in applying the electrical field properly in polycrystalline samples [52]. The ferroelectric properties of (H-quinine)$_2$Cu$_8$Cl$_{10}$ [51] and (H$_2$-quinine)$_2$Cu$_5$Cl$_9$ [20] reached a value of 0.12 and 0.28 µC cm^{-2} at a coercive filed of 5 and 16 kV cm^{-1}, respectively. Other hybrid metal halides with spherical organic molecules possessing low rotational energy barriers, such as quinuclidine, have been prepared in a thin film morphology, and their ferroelectric properties are comparable to those of $CnCoCl_3$ thin films. For example, thin films of complex salt 3-quinuclidinone cation and perchlorate anion (space group *Pna*2$_1$) showed a spontaneous polarization almost four times as high (P_s = 6.7 µC cm^{-2}) [53]. Since this material was deposited on a conductive ITO surface and contains GaIn eutectic top electrodes, it is comparable to the capacitor architecture used herein. Other comparable materials are thin films also deposited on ITO-coated substrates, such as quinuclidinium periodate (space group *Pmn*2$_1$, P_s = 7.71 µC cm^{-2}, E_c =255 kV cm^{-1}) [54], 3-oxoquinuclidinium tetrachlorocobaltate(II) (space group *P*2$_1$, P_s = 2.75 µC cm^{-2}, E_c =40 kV cm^{-1}) [31] and 4-fluoroquinuclidinium perrhenate (space group *Pn*, P_s = 11.2 µC cm^{-2}, E_c = 20 kV cm^{-1}) [55] for which theoretical calculations have confirmed the experimentally obtained value of spontaneous polarizations. In addition to the above-mentioned and well-established quinuclidine-based molecular ferroelectrics, these results demonstrate that natural alkaloids of the *Cinchona* family are also suitable homochiral and thermally stable organic molecules for the design and fabrication of soft molecular ferroelectric thin film capacitors.

3.4. Methanol sensing

Accurate and quantitative detection of methanol gas is required for industrial monitoring, fuel processing, methanol production, and food packaging safety testing [56]. Compared to conventional active materials for methanol gas detection, which are mainly composed of metal oxide semiconductors and operate at high temperatures (above 400 K), metal-organic materials offer advantages such as room temperature operation, selective detection in the sub-ppm range, chemical and structural tunability, and simple and environmentally-safe fabrication protocols [56–58]. The sensing properties of patterned $CnCoCl_3$ films with randomly distributed holes on the surface were investigated by exposing the films to methanol under atmospheric conditions (298 K, 1010 hPa, ~45% RH). For this purpose, gold electrodes with an area of 0.1 mm^2 were deposited on the top surface of the films and the in-

plane chronoamperometric current (at 10 V) was measured, as shown schematically in Figure 5b. The film was placed in a closed chamber and exposed to methanol by injecting a certain amount of the liquid, which evaporated in the chamber. Figure 5b shows that methanol vapor in the surrounding atmosphere strongly affects the electrical conductivity of the $CnCoCl_3$ thin films. After the addition of 100 ppm methanol, first a slight decrease and then a double increase of the current was observed. In order to achieve a faster recovery of the films after methanol exposure, the chamber was opened and dry nitrogen gas was introduced into the system so that the current reached the initial value. During the first cycle of methanol exposure, the current change is larger than in the following cycles, which is probably related to the faster uptake dynamics of methanol compared to desorption from the surface of the $CnCoCl_3$ films at ambient conditions. These proof-of-concept experiments have shown that patterned $CnCoCl_3$ thin films have prospects in methanol sensing applications. Further engineering of the $CnCoCl_3$ device could lead to better performing resistive gas sensors in terms of repeatability and faster response/recovery.

4. Conclusion

In this work, we have shown that it is possible to deposit thin films based on a homochiral natural *Cinchona* alkaloid and a chlorocobaltate(II) anion on various substrates (silicon, polypropylene, quartz and ITO-coated glass) using an environmentally friendly and facile dip-coating technique. Changing the deposition conditions of the dip-coating process has a significant influence on the crystallographic orientation and the morphology of the films. Completely dense and fully patterned films can be obtained. The relative humidity acts as a dewetting agent during the synthesis of the films and influences the simultaneous self-organization on the mesoscale, leading to the formation of random holes on the film surface. The synthesized films are thermally stable (up to 423 K) and their morphology is preserved during various sample manipulations. Spectroscopic and structural characterization confirmed the polar ferroelectric $P2_1$ structure of the films with a preferred [010] or [001] orientation and the single-phase nature of the films. The reason for the preferential crystal growth is directly related to the non-covalent interactions, a priori hydrogen bonds, which govern the self-assembly of the molecules during solvent evaporation. Dense films of cinchoninium-trichloro-cobalt(II) show a polarization switching of about 1.8 µC cm^{-2} at a coercive field of 50

kV cm^{-1} at room temperature, which is a good ferroelectric performance for a molecular ferroelectric material. The morphology of the fully patterned films is suitable for sensing applications due to the larger surface area, which has been demonstrated in the detection of methanol. Another possible functionality of these films is related to randomly distributed holes on the surface which could be useful in non-clonable surfaces and security applications. Altogether, this work shows a viable route for the fabrication and patterning of soft molecular thin films based on natural products that could be used for the development of solution-processed electronics.

CRediT authorship contribution statement

Mia Mesić: Samples growth and preparation, Performed measurements, Data analysis, Writing – review and editing. Lidija Androš Dubraja: Conceptualization, Funding acquisition, Data analysis, Supervision, Writing – original draft, review and editing.

Declaration of competing interest

The authors declare that they have no known competing financial interests or personal relationships that could have appeared to influence the work reported in this paper.

Data availability

Data is available from the authors upon reasonable request.

Acknowledgements

This work has been funded and supported by the Croatian Science Foundation Project No. UIP-2019-04-7433.

Appendix A. Supplementary data

Supplementary material associated with this article can be found, in the online version, at http:// dx.doi.org/…

References

[1] S. Horiuchi, Y. Tokunaga, G. Giovannetti, S. Picozzi, H. Itoh, R. Shimano, R. Kumai, Y. Tokura, Above-room-temperature ferroelectricity in a single-component molecular crystal, Nature 463 (2010) 789–792. https://doi.org/10.1038/nature08731

[2] D.-W. Fu, H.-L. Cai, Y. Liu, Q. Ye, W. Zhang, Y. Zhang, X.-Y. Chen, G. Giovannetti, M. Capone, J. Li, R.-G. Xiong, Diisopropylammonium Bromide Is a High-Temperature Molecular Ferroelectric Crystal, Science 339 (2013) 425–428. https://doi.org/10.1126/science.1229675

[3] Y. Ai, Y.-L. Zeng, W.-H. He, X.-Q. Huang, Y.-Y. Tang, Six-Fold Vertices in a Single-Component Organic Ferroelectric with Most Equivalent Polarization Directions, J. Am. Chem. Soc. 142 (2020) 13989–13995. https://doi.org/10.1021/jacs.0c06936

[4] Q. Pan, Z.-X. Gu, R.-J. Zhou, Z.-J. Feng, Y.-A. Xiong, T.-T. Sha, Y.-M. You, R.-G. Xiong, The past 10 years of molecular ferroelectrics: structures, design, and properties, Chem. Soc. Rev. 53 (2024) 5781–5861. https://doi.org/10.1039/D3CS00262D

[5] M. Dunatov, A. Puškarić, L. Androš Dubraja, Multi-stimuli responsive (L-tartrato)oxovanadium(V) complex salt with ferroelectric switching and thermistor properties, J. Mater. Chem. C 11 (2023) 2880–2888. https://doi.org/10.1039/D2TC05064A

[6] Z. Mallick, R. Sarkar, T. Kumar Kundu, D. Mandal, Molecular dipole regulated surface potential and ferroelectric characteristics in nanoconfined P(VDF-TrFE) architectures, Appl. Surf. Sci. 646 (2024) 158925. https://doi.org/10.1016/j.apsusc.2023.158925

[7] H. S. Choi, S. Li, I.-H. Park, W. H. Liew, Z. Zhu, K. C. Kwon, L. Wang, I.-H. Oh, S. Zheng, C. Su, Q.-H. Xu, K. Yao, F. Pan, K. P. Loh, Tailoring the coercive field in ferroelectric metal-free perovskites by hydrogen bonding, Nat Commun. 13 (2022) 794. https://doi.org/10.1038/s41467-022-28314-8

[8] C.-C. Fan, C.-D. Liu, B.-D. Liang, W. Wang, M.-L. Jin, C.-Y. Chai, C.-Q. Jing, T.-Y. Ju, X.-B. Han, W. Zhang, Tuning ferroelectric phase transition temperature by enantiomer fraction, Nat Commun. 15 (2024) 1464. https://doi.org/10.1038/s41467-024-45986-6

[9] Z.-J. Feng, Y.-A. Xiong, W.-C. Sun, T.-T. Sha, J. Yao, Q. Pan, H. Hu, S. Dong, R.-G. Xiong, Y.-M. You, First Observation of Negative Capacitance in Molecular Ferroelectric Thin Films, Adv. Mater. 36 (2024) 2307518. https://doi.org/10.1002/adma.202307518

[10] Y. Sekine, R. Akiyoshi, S. Hayami, Recent advances in ferroelectric metal complexes, Coord. Chem. Rev. 469 (2022) 214663. https://doi.org/10.1016/j.ccr.2022.214663

[11] M. Mon, J. Ferrando-Soria, M. Verdaguer, C. Train, C. Paillard, B. Dkhil, C. Versace, R. Bruno, D. Armentano, E. Pardo, Postsynthetic Approach for the Rational Design of Chiral Ferroelectric Metal–Organic Frameworks, J. Am. Chem. Soc. 139 (2017) 8098–8101. https://doi.org/10.1021/jacs.7b03633

[12] Y.-A. Xiong, S.-S. Duan, H.-H. Hu, J. Yao, Q. Pan, T.-T. Sha, X. Wei, H.-R. Ji, J. Wu, Y.-M. You, Enhancement of phase transition temperature through hydrogen bond modification in molecular ferroelectrics, Nat Commun. 15 (2024) 4470. https://doi.org/10.1038/s41467-024-48948-0

[13] J. Lewiński, T. Kaczorowski, I. Justyniak, D. Prochowicza, Development of chiral N,N-ditopic metalloligands based on a Cinchona alkaloids' backbone for constructing homochiral coordination polymers, Chem. Commun. 47 (2011) 950–952. https://doi.org/10.1039/C0CC03586F

[14] H. Martin, R. Hoffmann, J. Frackenpohl, Recent Advances in Cinchona Alkaloid Chemistry, Eur. J. Org. Chem. (2004) 4293–4312. https://doi.org/10.1002/ejoc.200400294

[15] I. Hisaki, E. Hiraishi, T. Sasaki, H. Orita, S. Tsuzuki, N. Tohnai, M. Miyata, Crystal Structure of Quinine: The Effects of Vinyl and Methoxy Groups on Molecular Assemblies of Cinchona Alkaloids Cannot Be Ignored, Chem. Asian J. 7 (2012) 2607–2614. https://doi.org/10.1002/asia.201200566

[16] J. Achan, A. O. Talisuna, A. Erhart, A. Yeka, J. K. Tibenderana, F. N. Baliraine, P. J. Rosenthal, U. D'Alessandro, Quinine, an old anti-malarial drug in a modern world: role in the treatment of malaria, Malar. J. 10 (2011) 144. https://doi.org/10.1186/1475-2875-10-144

[17] S. Zheng, C. M. Schienebeck, W. Zhang, H.-Y. Wang, W. Tang, Cinchona Alkaloids as Organocatalysts in Enantioselective Halofunctionalization of Alkenes and Alkynes, Asian J. Org. Chem. 3 (2014) 366–376. https://doi.org/10.1002/ajoc.201400030

[18] T. Kaczorowski, I. Justyniak, T. Lipińska, J. Lipkowski, J. Lewiński, Metal Complexes of Cinchonine as Chiral Building Blocks: A Strategy for the Construction of Nanotubular Architectures and Helical Coordination Polymers, J. Am. Chem. Soc. 131 (2009) 5393–5395. https://doi.org/10.1021/ja8098867

[19] H.-L. Cai, T. Zhang, L.-Z. Chen, R.-G. Xiong, The first homochiral compound with temperature-independence of piezoelectric properties, J. Mater. Chem. 20 (2010) 1868–1870. https://doi.org/10.1039/B926053F

[20] H. Zhao, Z.-R. Qu, Q. Ye, B. F. Abrahams, Y.-P. Wang, Z.-G. Liu, Z. Xue, R.-G. Xiong, X.-Z. You, Ferroelectric Copper Quinine Complexes, Chem. Mater. 15 (2003) 4166–4168. https://doi.org/10.1021/cm034301u

[21] H.-Y. Ye, Y.-Y. Tang, P.-F. Li, W.-Q. Liao, J.-X. Gao, X.-N. Hua, H. Cai, P.-P. Shi, Y.-M. You, R.-G. Xiong, Metal-free three-dimensional perovskite ferroelectrics, Science 361 (2018) 151. https://doi.org/10.1126/science.aas9330

[22] A. Skórska, B. J. Oleksyn, J. Śliwiński, Cobalt Complex of Cinchonine: Intermolecular Interactions in Two Crystalline Modifications, Enantiomer 7 (2010) 295–303. https://doi.org/10.1080/10242430215706

[23] X.-X. Cao, R.-J. Zhou, Y.-A. Xiong, G.-W. Du, Z.-J. Feng, Q. Pan, Y.-Z. Chen, H.-R. Ji, Z. Ni, J. Lu, H. Hu, Y.-M. You, Volume-Confined Fabrication of Large-Scale Single-Crystalline Molecular Ferroelectric Thin Films and Their Applications in 2D Materials, Adv. Sci. (2023) 2305016. https://doi.org/10.1002/advs.202305016

[24] R. Acharya, B. Peng, P. K. L. Chan, G. Schmitz, H. Klauk, Achieving Ultralow Turn-On Voltages in Organic Thin-Film Transistors: Investigating Fluoroalkylphosphonic Acid Self-Assembled Monolayer Hybrid Dielectrics, ACS Appl. Mater. Interfaces 11 (2019) 27104–27111. https://pubs.acs.org/doi/10.1021/acsami.9b04361

[25] Z. Wang, S. Wang, L. Huang, L. Li, L. Chi, Microstructured Ultrathin Organic Semiconductor Film via Dip-Coating: Precise Assembly and Diverse Applications, Acc. Mater. Res. 1 (2020) 201–212. https://doi.org/10.1021/accountsmr.0c00042

[26] M. Yang, T. Zhang, P. Schulz, Z. Li, G. Li, D. H. Kim, N. Guo, J. J. Berry, K. Zhu, Y. Zhao, Facile fabrication of large-grain $CH_3NH_3PbI_{3-x}Br_x$ films for high-efficiency solar cells via CH_3NH_3Br-selective Ostwald ripening, Nat. Commun. 7 (2016) 12305. https://doi.org/10.1038/ncomms12305

[27] M. Cinquino, M. Pugliese, C. T. Prontera, F. Mariano, A. Zizzari, G. Maiorano, A. Maggiore, R. Manfredi, C. Mello, I. Tarantini, G. Gigli, V. Maiorano, Inkjet-printed multilayer structure for low-cost and efficient OLEDs, J. Sci. Adv. Mater. Devices 9 (2024) 100707. https://doi.org/10.1016/j.jsamd.2024.100707.

[28] E. Melito, A. Laventure, G. Aldea-Nunzi, C. Pellerin, E. Buncel, O. Lebelc, J.-M. Nunzi, Water-triggered spontaneous surface patterning in thin films of mexylaminotriazine molecular glasses, J. Mater. Chem. C 3 (2015) 4729–4736. https://doi.org/10.1039/C4TC01845A

[29] E. Destouesse, S. Chambon, S. Courtel, L. Hirsch, G. Wantz, Solution processed small molecule bulk heterojunctions: leakage currents and the dewetting issue for inverted solar cells, ACS Appl. Mater. Interfaces 7 (2015) 24663–24669. https://doi.org/10.1021/acsami.5b06964

[30] P.-Y. Chung, M.-H. Cheng, H.-F. Tseng, C.-T. Liu, T.-Y. Chiu, K.-S. Jeng, M.-H. Chi, J.-T. Chen, Dewetting of Swollen Poly(3-hexylthiophene) Films during Spin-Coating Processes: Implications for Device Fabrication, ACS Appl. Nano Mater. 1 (2018) 2021–2028. https://doi.org/10.1021/acsanm.8b00201

[31] M. Mesić, M. Dunatov, A. Puškarić, Z. Štefanić, L. Androš Dubraja, Humidity and temperature driven transformations in ferroelectric quinuclidine-based chlorocobaltate(ii) complex salt: bulk and thin films with preferred orientation, J. Mater. Chem. C 12 (2024) 12397–12404. https://doi.org/10.1039/D4TC01150C

[32] E. A. Gaulding, B. T. Diroll, E. D. Goodwin, Z. J. Vrtis, C. R. Kagan, C. B. Murray, Deposition of Wafer-Scale Single-Component and Binary Nanocrystal Superlattice Thin Films Via Dip-Coating, Adv. Mater. 27 (2015) 2846–2851. https://doi.org/10.1002/adma.201405575

[33] G. Reiter, Dewetting of Thin Polymer Films, Phys. Rev. Lett. 68 (1992) 75. https://doi.org/10.1103/PhysRevLett.68.75

[34] G. Reiter, Unstable Thin Polymer Films: Rupture and Dewetting Processes, Langmuir 9 (1993) 1344–1351. https://doi.org/10.1021/la00029a031

[35] J. Becker, G. Grün, R. Seemann, H. Mantz, K. Jacobs, K. R. Mecke, R. Blossey, Complex dewetting scenarios captured by thin-film models, Nature Mater. 2 (2003) 59–63. https://doi.org/10.1038/nmat788

[36] E. Seyedhosseini, K. Romanyuk, D. Vasileva, S. Vasilev, A. Nuraeva, P. Zelenovskiy, M. Ivanov, A. N. Morozovska, V. Y. Shur, H. Lu, Self-assembly of Organic Ferroelectrics by Evaporative Dewetting: A Case of β-Glycine, ACS Appl. Mater. Interfaces 9 (2017) 20029−20037. https://doi.org/10.1021/acsami.7b02952

[37] M. Cavallini, J. Gomez-Segura, C. Albonetti, D. Ruiz-Molina, J. Veciana, F. Biscarini, Ordered Patterning of Nanometric Rings of Single Molecule Magnets on Polymers by Lithographic Control of Demixing, J. Phys. Chem. B 110 (2006) 24. https://doi.org/10.1021/jp061231g

[38] J.-N. Tisserant, G. Wicht, O. F. Göbel, E. Bocek, G.-L. Bona, T. Geiger, R. Hany, R. Mezzenga, S. Partel, P. Schmid, W. B. Schweizer, J. Heier, Growth and Alignment of Thin Film Organic Single Crystals from Dewetting Patterns, ACS Nano 7 (2013) 5506–5513. https://doi.org/10.1021/nn401679s

[39] P. Zaumseil, High-resolution characterization of the forbidden Si 200 and Si 222 reflections, J. Appl. Cryst. 48 (2015) 528–532. https://doi.org/10.1107/S1600576715004732

[40] Z.-Z. Ma, Q.-H. Li, Z. Wang, Z.-G. Gu, J. Zhang, Electrically regulating nonlinear optical limiting of metal-organic framework film. Nat Commun 13 (2022) 6347. https://doi.org/10.1038/s41467-022-34139-2

[41] A. E. Özel, Y. Büyükmurat, S. Akyüz, Infrared-spectra and normal-coordinate analysis of quinoline and quinoline complexes, J. Mol. Struct. 565–566 (2001) 455–462. https://doi.org/10.1016/S0022-2860(00)00793-6

[42] C. Decaroli, A. M. Arevalo-Lopez, C. H. Woodall, E. E. Rodriguez, J. P. Attfield, S. F. Parker, C. Stock, $(C_4H_{12}N_2)[CoCl_4]$: tetrahedrally coordinated Co^{2+} without the orbital degeneracy, Acta Cryst. B71 (2015) 20–24. https://doi.org/10.1107/S2052520614024809

[43] J. Hwang, N. Shoji, A. Endo, H. Daiguji, Effect of Withdrawal Speed on Film Thickness and Hexagonal Pore-Array Dimensions of SBA-15 Mesoporous Silica Thin Film, Langmuir 30 (2014) 15550–15559. https://doi.org/10.1021/la5037713

[44] M. Dunatov, K. Molčanov, Z. Štefanić, R. Kruk, L. Androš Dubraja, Interfacial Water Molecules as Agents for Phase Change Control and Proton Conductivity Enhancement

in the Ammonium Vanadyl Tartrate System, Inorg. Chem. 63 (2024) 163−172. https://doi.org/10.1021/acs.inorgchem.3c02605

[45] N. Torun, I. Torun, M. Sakir, M. Kalay, M. S. Onses, Physically Unclonable Surfaces via Dewetting of Polymer Thin Films, ACS Appl. Mater. Interfaces 13 (2021) 11247–11259. https://doi.org/10.1021/acsami.0c16846

[46] S. Goswami, I. Hod, J. D. Duan, C. W. Kung, M. Rimoldi, C. D. Malliakas, R. H. Palmer, O. K. Farha, J. T. Hupp, Anisotropic Redox Conductivity within a Metal–Organic Framework Material, J. Am. Chem. Soc. 141 (2019) 17696–17702. https://doi.org/10.1021/jacs.9b07658

[47] A. Roy, R. Prasad, S. Auluck, A. Garg, Engineering polarization rotation in ferroelectric bismuth titanate, Appl. Phys. Lett. 102 (2013) 182901. https://doi.org/10.1063/1.4804367

[48] P. R. Spackman, M. J. Turner, J. J. McKinnon, S. K. Wolff, D. J. Grimwood, D. Jayatilaka, M. A. Spackman, CrystalExplorer: a program for Hirshfeld surface analysis, visualization and qu-antitative analysis of molecular crystals. J. Appl. Cryst. 54 (2021) 1006–1011. 10.1107/S1600576721002910

[49] J. F. Scott, L. Kammerdiner, M. Parris, S. Traynor, V. Ottenbacher, A. Shawabkeh, W. F. Oliver, Switching kinetics of lead zirconate titanate submicron thin-film memories, J. Appl. Phys. 4 (1988) 787–792. https://doi.org/10.1063/1.341925

[50] V. Bornand, S. Trolier-McKinstry, K. Takemura, C. A. Randall, Orientation dependence of fatigue behavior in relaxor ferroelectric–PbTiO3 thin films, J. Appl. Phys. 87 (2000) 3965–3972. https://doi.org/10.1063/1.372442

[51] Z.-R. Qu, Z.-F. Chen, J. Zhang, R.-G. Xiong, B. F. Abrahams, Z.-L. Xue, The First Highly Stable Homochiral Olefin-Copper(I) 2D Coordination Polymer Grid Based on Quinine as a Building Block, Organometallics 22 (2003) 2814–2816. https://doi.org/10.1021/om030134w

[52] L. Androš Dubraja, R. Kruk, T. Brezesinski, Robust Macroscopic Polarization of Block Copolymer–Templated Mesoporous Perovskite-Type Thin-Film Ferroelectrics, Adv. Electron. Mater. 5 (2019) 1800287. https://doi.org/10.1002/aelm.201800287

[53] C.-K. Yang, W.-N. Chen, Y.-T. Ding, J. Wang, Y. Rao, W.-Q. Liao, Y. Xie, W. Zou, R.-G. Xiong, Directional Intermolecular Interactions for Precise Molecular Design of a High-T_c Multiaxial Molecular Ferroelectric, J. Am. Chem. Soc. 141 (2019) 1781–1787. https://doi.org/10.1021/jacs.8b13223

[54] Y.-M. You, Y.-Y. Tang, P.-F. Li, H.-Y. Zhang, W.-Y. Zhang, Y. Zhang, H.-Y. Ye, T. Nakamura, R.-G. Xiong, Quinuclidinium salt ferroelectric thin-film with duodecuple-rotational polarization-directions, Nature comm. 8 (2017) 14934. https://doi.org/10.1038/ncomms14934

[55] Y.-Y. Tang, Y. Xie, W.-Q. Liao, P.-F. Li, T. Nakamura, R.-G. Xiong, Organic Ferroelectric Vortex–Antivortex Domain Structure, J. Am. Chem. Soc. 142 (2020) 21932–21937. https://doi.org/10.1021/jacs.0c11416

[56] F. Dai, X. Cui, Y. Luo, D. Zhang, N. Li, Y. Huang, Y. Peng, Ultrathin MOF nanosheet-based resistive sensors for highly sensitive detection of methanol. Chem, Commun. 58 (2022) 11543–115546. https://doi.org/10.1039/D2CC04230D

[57] M. S. Hosseini, S. Zeinali, M. H. Sheikhi, Fabrication of Capacitive Sensor Based on Cu-BTC (MOF-199) Nanoporous Film for Detection of Ethanol and Methanol Vapors, Sensor. Actuator. B Chem. 230 (2016) 9–16. https://doi.org/10.1016/j.snb.2016.02.008

[58] Z. Zhai Yaxin Sun, X. Hao, C. Li, Capacitive gas sensors based on a ZIF-67/PAN nanofiber membrane to detect volatile organic compounds, Appl. Surf. Sci. 621 (2023) 156833. https://doi.org/10.1016/j.apsusc.2023.156833